Characterization in bi-parameter space of a non-ideal oscillator

S. L. T. de Souza[1,2,*], A. M. Batista[2,3], M. S. Baptista[4], I. L. Caldas [2] and J. M. Balthazar[5]

[1] *Departamento de Física e Matemática, Universidade Federal de São João del-Rei, Caixa Postal 131, 36420-000, Ouro Branco, MG, Brazil*

[2] *Instituto de Física, Universidade de São Paulo, 05315-970, São Paulo, SP, Brazil*

[3] *Departamento de Matemática e Estatística, Universidade Estadual de Ponta Grossa, 84030-900, Ponta Grossa, PR, Brazil*

[4] *Institute for Complex Systems and Mathematical Biology, SUPA, University of Aberdeen, AB24 3UE Aberdeen, United Kingdom*

[5] *ITA (Aeronautics Technological Institute), Mechanical-Aeronautics Division, 12228-900, São José dos Campos, SP, Brazil*

Abstract

We investigate the dynamical behavior of a non-ideal Duffing oscillator, a system composed of a mass-spring-pendulum driven by a DC motor with limited power supply. To identify new features on Duffing oscillator parameter space due to the limited power supply, we provide an extensive numerical characterization in the bi-parameter space by using Lyapunov exponents. Following this procedure, we identify remarkable new organized distribution of periodic windows, the ones known as Arnold tongues and also shrimp-shaped structures. In addition, we also identify intertwined basins of attraction for coexisting multiple attractors connected with tongues.

Keywords: Chaos, Arnold tongues, shrimp-shaped structures, coupled oscillators

1. Introduction

In recent years, there has been an increasing amount of work on nonlinear dynamics characterizing the possible structures in two-dimensional control parameter (bi-parameter) space [1]. Accordingly, periodic windows with important features, mainly shrimp-shaped structures [2] and Arnold tongues [3, 4, 5], have been identified in several systems such as two-gene model [6], impact oscillator [7, 8], dissipative model of relativistic particles [9], tumor growth model [10], Chua's circuit [11, 12, 13], prey-predator model [14], and Red Grouse population model [15].

In the nonlinear dynamics context, oscillators with mechanical coupling have recently attracted a significant attention due to the complexity of the dynamics for high degree-of-freedom devices and possible applications to advanced technologies [16, 17, 18, 19, 20]. Among the class of mechanical coupling oscillators an interesting example is the mass-spring-pendulum system [21, 22]. Svoboda and collaborators studied a system of masses with a pendulum, where the pendulum is attached to one mass of a chain of masses connected by springs [23]. They showed that autoparametric resonance can arise. In Reference [24] was investigated the influence of nonlinear

---

*Corresponding author: thomaz@ufsj.edu.br

spring on the auto parametric system. It was verified the existence of rich dynamics such as chaotic oscillations.

In this work, we investigate the parameter space organization of a non-ideal Duffing oscillator, namely, the mass-spring-pendulum system. Duffing oscillator is a forced oscillator with a nonlinear elasticity, and it is described by a non linear differential equation of second-order that has been used in a variety of physical processes. This oscillator is well known in engineering science, and it has been used to model the dynamics of types of electrical and mechanical systems. Almong and collaborators experimentally studied signal amplification in a nanomechanical Duffing resonator via stochastic resonance [25]. The Duffing oscillator is also a useful model to study the dynamics behavior of structural systems, such as columns, gyroscopes, and bridges [26].

The non-ideal character of the studied oscillator is a consequence of the fact that the source of energy is given by a DC motor with limited power supply [27, 28]. Previous studies of this system have shown a rich dynamical behavior with several nonlinear phenomena, like quasi-periodic attractors, chaotic regimes, crises, coexistence of attractors, and fractal basin boundaries [29, 30, 31]. Here, our main purpose is to provide a global parameter analysis of the behavior of this oscillator with a mechanical coupling. The main features found in the parameter space were the self-similar structures, such as shrimps and Arnold tongues. Comparing with results from parameter spaces of ideal oscillators, these Arnold tongue attributes are a consequence of the non-ideal character of this oscillator.

This paper is organized as follows. In Section 2 we present the mathematical description of the non-ideal Duffing oscillator. In Section 3, we provide characterization of the periodic windows identified in the bi-parameter space. In section 4, we also provide an example of a possible coexistence of multiple attractors and their corresponding basins of attraction. The last section contains our main conclusions.

2. Non-ideal Duffing oscillator

Several mechanical systems can be described by the Duffing equation. Tusset and Balthazar [32] studied ideal and non-ideal Duffing oscillator with chaotic behavior. They suppressed the chaotic oscillations through the application of two control signals. In this work, we consider a non-ideal system consisting of a mass, spring and pendulum. Figure 1 shows a schematic model of the non-ideal oscillator [31], that is composed of a cart (mass M), with a pendulum (mass m and length r), connected to a fixed frame by a nonlinear spring and a dash-pot. We denote by X the displacement of the cart and by φ the angular displacement of the pendulum.

The equations of motion, obtained by using Lagrangian approach, for both the cart and the pendulum are given by:

$$(m + M)\frac{d^2 X}{dt^2} + c_1\frac{dX}{dt} - k_1 X + k_2 X^3 = mr\left(\frac{d\varphi}{dt}^2 \sin\varphi - \frac{d^2\varphi}{dt^2}\cos\varphi\right), \tag{1}$$

$$mr^2\frac{d^2\varphi}{dt^2} + c_2\frac{d\varphi}{dt} + mgr\sin\varphi = E - mr\frac{d^2 X}{dt^2}\cos\varphi, \tag{2}$$

where E is a constant source of energy. According to Equation (1), for $k_1 < 0$, the Duffing oscillator can be interpreted as a forced oscillator with a spring whose restoring force is $F = k_1 X - k_2 X^3$. Whereas, for $k_1 > 0$, the Duffing oscillator describes the dynamics of a point mass in a double well potential, such as a deflection structure building model.
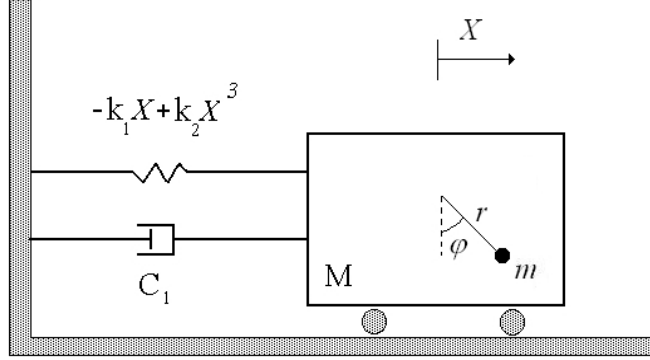
Figure 1: Schematic model of the non-ideal oscillator.

Considering $x \equiv X/r$ and $\tau \equiv \omega_1 t$ $(\omega_1 \equiv \sqrt{\frac{k_1}{m+M}})$, the equations of motion are rewritten in the following form:

$$\ddot{x} + \beta_1 \dot{x} - x + \gamma x^3 = \varepsilon \left(\dot{\varphi}^2 \sin \varphi - \ddot{\varphi} \cos \varphi \right), \tag{3}$$

$$\ddot{\varphi} + \beta_2 \dot{\varphi} + \Omega^2 \sin \varphi = \alpha - \ddot{x} \cos \varphi. \tag{4}$$

for $\beta_1 \equiv \frac{c_1}{(m+M)\omega_1}$, $\gamma \equiv \frac{k_2}{k_1} r^2$, $\varepsilon \equiv \frac{m}{m+M}$, $\beta_2 \equiv \frac{c_2}{mr^2\omega_1^2}$, $\Omega \equiv \frac{\omega_2}{\omega_1}$ $(\omega_2 \equiv \sqrt{g/r})$, and $\alpha \equiv \frac{E}{mr^2\omega_1^2}$ (source of energy).

These equations of motion correspond to a simplified mathematical model for oscillator with a limited power supply. In this case, the source of energy is given by a DC motor and the parameter α is associated with its input voltage.

3. Arnold tongues and Shrimps

In this Section, we present numerical results identifying periodic windows in bi-parameter space for the non-ideal Duffing oscillator. The simulations were performed by using the fourth-order Runge-Kutta method with a fixed step. The control parameters were fixed at $\beta_1 = 0.05$, $\beta_2 = 1.5$, $\gamma = 0.1$, and $\Omega = 1.0$. We consider for dynamic investigations the variations of parameters ε (the ratio of the masses) and α (input voltage of the DC motor).

First, we use a bifurcation diagram, as shown in Figures 2(a) and (b) for $\varepsilon = 0.09$, to verify possible solutions generated by the oscillator. This diagram is constructed varying the control parameter α. For each value of the parameter, we plot the local maximum values of the dynamical variable x neglecting the transients. As can be seen in Figure 2(b), the bifurcation diagram is composed of periodic windows associated with period-adding sequence. See as an example the three main periodic windows in (b), with periodic attractor of periods 5, 4, and 3. Then, as α is increased the period decreases by 1.

In addition, Figure 2(a) exhibits the coexistence of two attractors each one plotted with a different color (black and blue). In mechanical systems, the coexistence of attractors is common non-linear phenomenon. For example, the coexistence of a large number of periodic attractors in a mechanical system was observed by Feudel and collaborators [33]. They studied the kicked

double rotor system, and verified the possibility of the system to be stabilized by means of a small perturbation. In an experimental nonlinear pendulum, it was also observed two coexisting attractors [34]. Multiple attractors may be found in many nonlinear dynamical systems, for instance, driven damped pendulum [35], spring-pendulum system [36], and impact oscillators [37, 38].
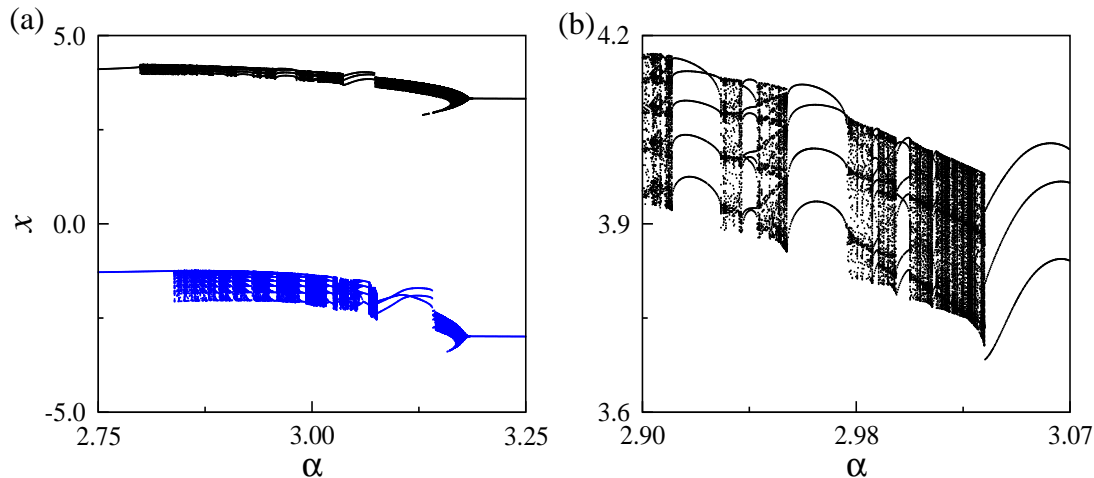

Figure 2: (Color online) (a) Bifurcation diagram showing coexisting attractors for x in terms of α with $\varepsilon = 0.09$. (b) Magnification of bifurcation diagram for the attractors plotted in black.

In order to better characterize the dynamics of the oscillator and to examine the structures related to the periodic windows, we construct diagrams of two-dimensional parameter space (bi-parameter space) by using the Lyapunov exponents. To evaluate these exponents, we use the algorithm proposed by Wolf and collaborators [39]. One positive Lyapunov exponent (LLE) indicates a chaotic attractor, all negative exponents (excluding one null exponent) a periodic, and two null exponents a quasi-periodic or a bifurcation point.

Figures 3(a)-(d) present the parameter plane diagrams, for ε *versus* α (mass ratio *versus* source of energy), using a grid of 800×800 cells. Periodic solutions are plotted in blue, green and black scale ranges, quasi-periodic in red (bifurcation points in red), and chaotic in white, where the colors, corresponding to range of Lyapunov exponents values, are introduced to emphasize the structure details.

In Figure 3(b), we provide a magnification of rectangular area (yellow box) of Figure 3(a) revealing many periodic structures (in black) knowing as Arnold tongues [6] that correspond to phase locking, i.e., periodic orbits with the same frequency. Surprisingly, the tongues origins appear for low value of ε for a given α, accumulate in a starting point, namely, the tongues distributions appear highly organized. Moreover, we can observe in Figures 3(c) and (d) small periodic structures (blue, green, and black), named shrimps [2], embedded in parameter regions with chaotic regimes (white). The shrimps are composed of the central body bordered by a saddle-node and a flip bifurcations.

For further analysis of the Arnold tongue organization, we evaluate the period of the attractors as shown in Figure 4(a) (a partial magnification of Fig. 3b) identifying a period-adding sequence for the tongues with accumulation on period-1 region. The period of the sequence increases by 1 ($3 \rightarrow 4 \rightarrow 5 \rightarrow 6 \rightarrow \cdots$), which is the same period of the accumulation structure. It was
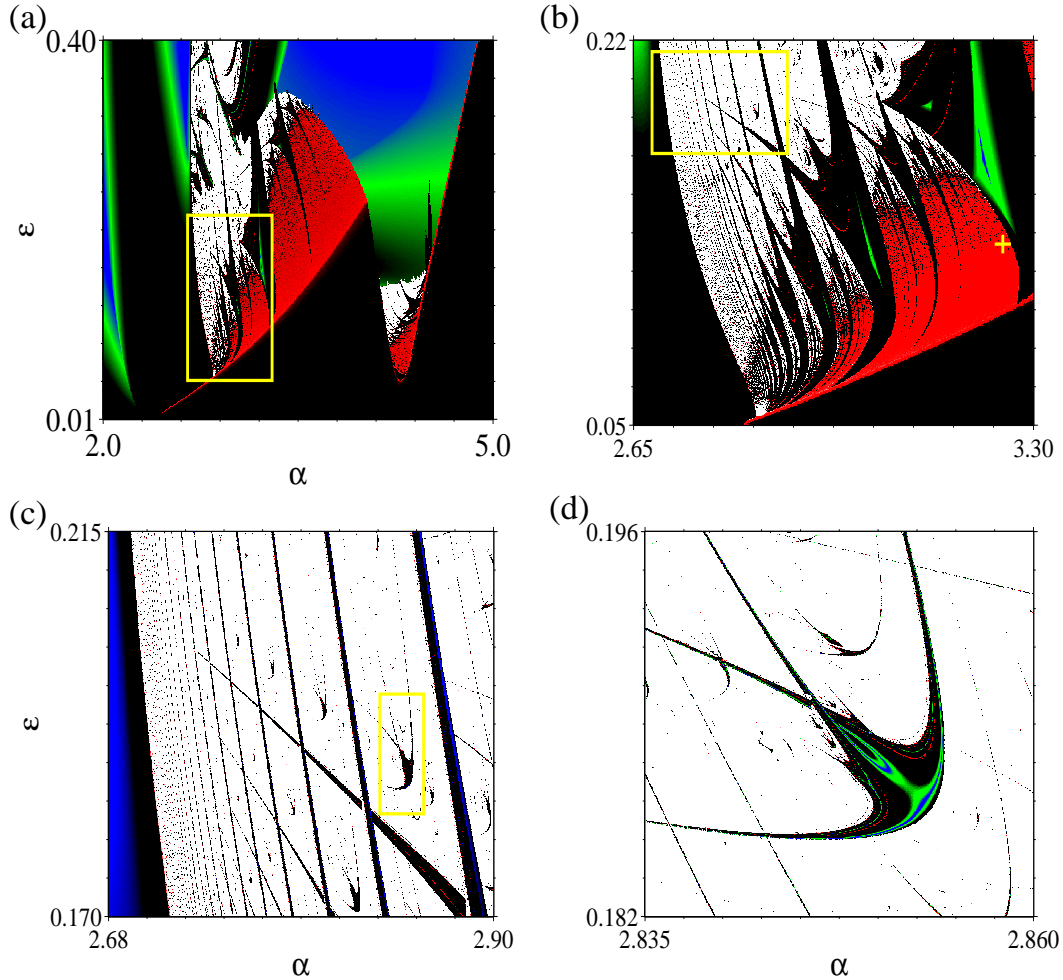
Figure 3: (Color online) (a) Parameter plane diagram for ε versus α. Periodic solutions are plotted in blue, green and black scale ranges, quasi-periodic in red, and chaotic in white. (b)-(d) Successive magnifications of boxes in yellow shown in (a,b,c).

considered the tongue size to identify the sequence. Following the dashed line indicated in Figure 4(a), we show a bifurcation diagram in Figure 5(a) providing a better view of this period-adding sequence. Another example of period-adding sequence can be seen from parameter plane and bifurcation diagrams depicted in Figures 4(b) and 5(b), respectively. In this example, the period of the sequence increases by 3 ($7 \rightarrow 10 \rightarrow 13 \rightarrow \cdots$). In fact, a considerable quantities of sequences can be identified in regions of the parameter space associated with tongues, that play a role of acummulation structures. The adding rules correspond to period of these acummulation structures.

Moreover, Figures 4(a)-(d) show a possible Fibonacci-like sequence (number in red) associated with the period of the tongues. Each new term of the Fibonacci-like sequence is obtained by the sum of two previous ones. Therefore, starting with periods 3 and 4 (Fig. 4a), this sequence is composed of the numbers: $3 \rightarrow 4 \rightarrow 7 \rightarrow 11 \rightarrow 18 \rightarrow 29 \rightarrow \cdots$.

In Figures 6(a) and (b), we explore an apparent property for the shrimp-shaped structures. For that purpose, we consider the shrimp plotted (in black) in Figure 4(a) with label 7. We
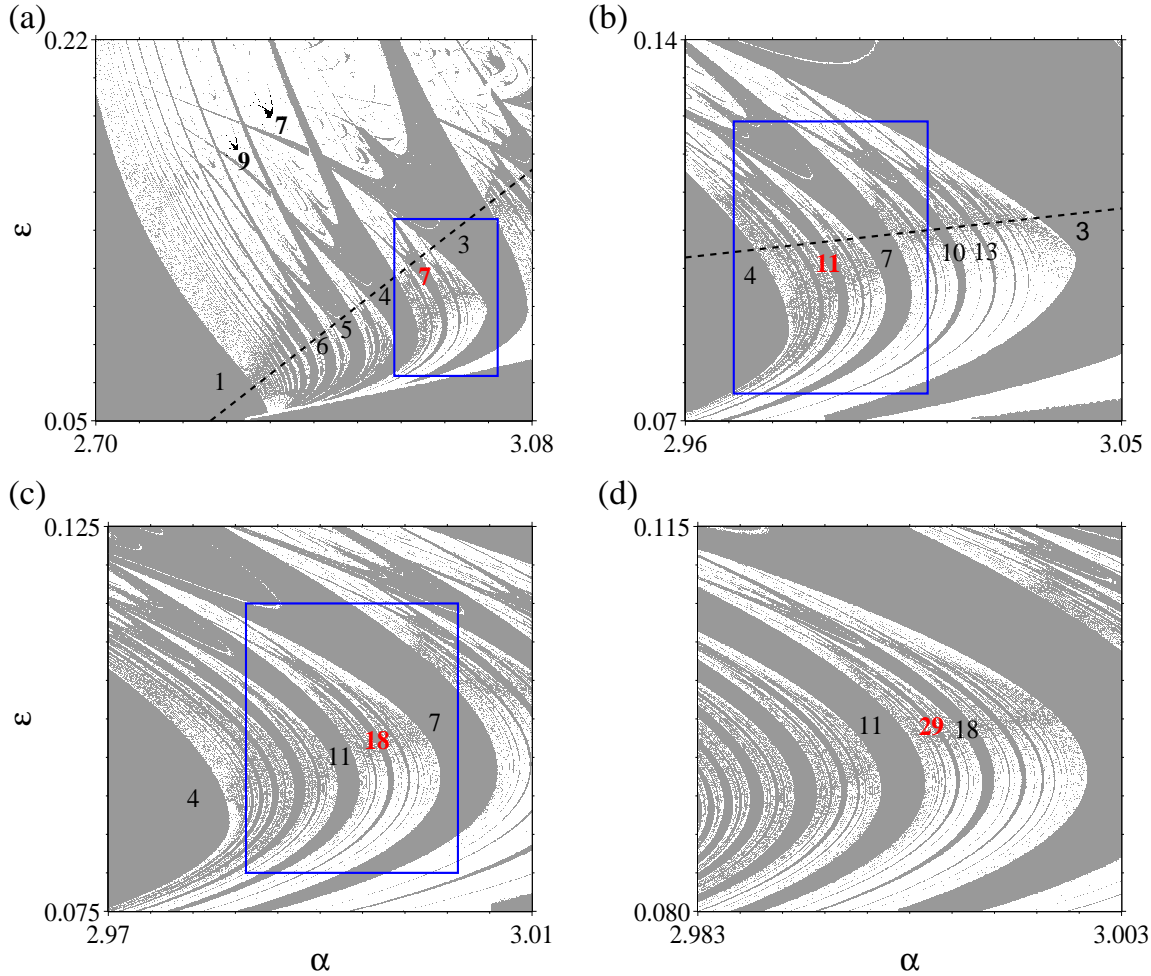
5

Figure 4: (Color online) (a) Parameter plane diagram for ε *versus* α. Periodic solutions are plotted in light gray. (b)-(d) Successive magnifications of boxes in blue shown in (a,b,c).

evaluate the periodicity of this stucture (Fig. 6a) and the associated largest secondary shrimps (Fig. 6b) observed close of this main one. The main shrimp has period-7 and the secondary one has period-21, that is three times the period of the main structure. The same signature, evidencing period-3x windows, was firstly reported for a discrete-time system named two-gene model [6].

4. Coexistence of multiple attractors and basins of attraction

For this type nonideal oscillator, de Souza and collaborators reported coexistence of attractors [31], that is multiple solutions for the same set of control parameters. In this reported case, basins of attraction exhibited fractal boundaries (basin of attraction is the set of initial conditions leading, after a transient behavior, to a specific attractor). Magnifications of the fractal boundary regions reveal an arbitrarily fine-scaled structure with final state sensitivity due to possible small uncertainties in the initial conditions. An interesting description of fractal basin boundaries and their corresponding features can be found in the reference [40].
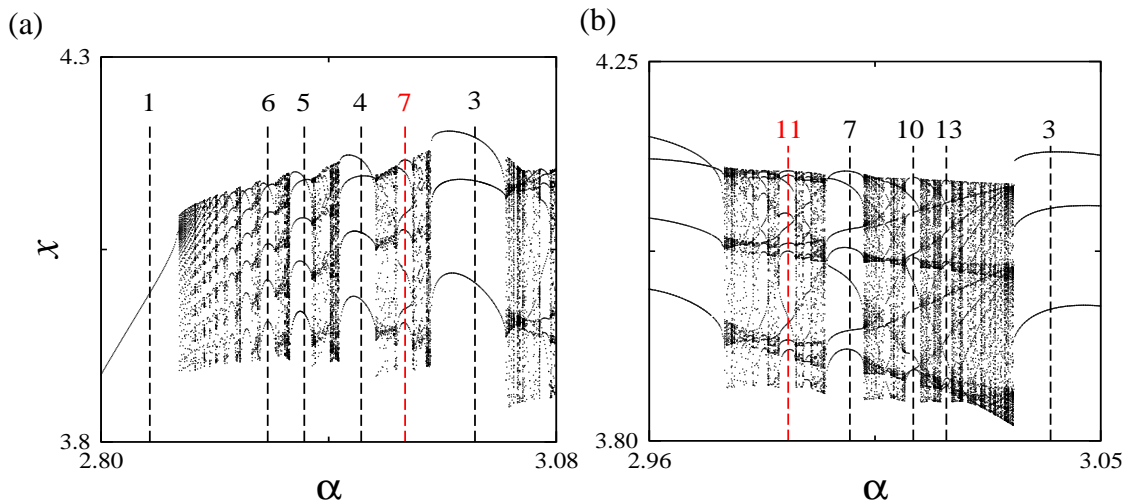
Figure 5: (Color online) Bifurcation diagrams for x in terms of α with (a) $\varepsilon = 0.4\alpha - 1.08$ (dashed line shown in Fig. 4a) and (b) $\varepsilon = 0.1\alpha - 0.196$ (dashed line shown in Fig. 4b).
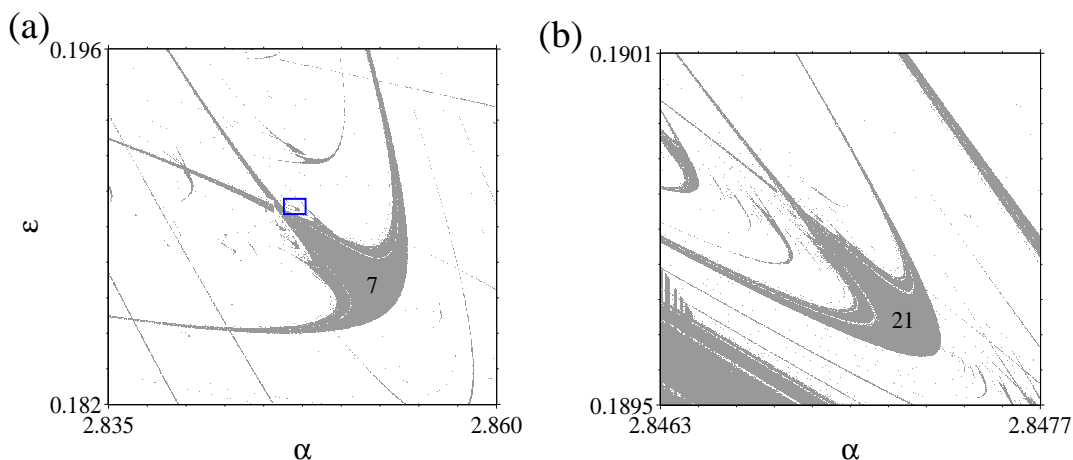

Figure 6: (Color online) (a) Parameter plane diagram showing magnification of the periodic structure with period 7 plotted in black in Fig. 4(a). (b) Magnification of box in blue shown in (a).

Here, we present coexistence of multiple attractors with a different type of basins of attraction reported for this oscillator. These basins possess a peculiar structure named intertwined basins by Grebogi and collaborators [41]. Figure 7 shows the phase portraits of two periodic and two quasi-periodic attractors for $\alpha = 3.25$ and $\varepsilon = 0.13$. Lyapunov exponents used to characterize these attractors are not shown here. These parameters are at the border between a red (quasi-periodic attractor) and a black area (periodic attractor) indicated by a yellow cross in Figure 3(b). For these parameters both attractors observed for $x > 0$ in Figure 7 coexist and they show up depending on the way we follow the attractor in such hysteresis area. The same is valid for the other two attractors observed in Figure 7 for $x < 0$. In fact, hysteresis area with coexistence of attractors is apparently one more property associated with tongues. This phenomenon of coexisting attractors connected with tongues was also reported by X. Xu and collaborators for a parametrically-excited pendulum [42].

The corresponding basins of attraction of these possible oscillations are depicted in Figures

7

8(a)-(d) with the same color used for the attractors in Figure 7. This diagram of basins is constructed using a grid of 1000×1000 equally spaced cells as set of initial conditions for velocity $\dot{x}$ in terms of displacement x. The basins have a complex shape with boundaries convoluted and apparently fractal as shown in Figures 8(a) and (c). However, the boundaries are composed of smooth curves as depicted in Figure 8(b) and (d) for boundaries of basins plotted in black and red (Fig. 8b) and for blue and green (Fig. 8d).
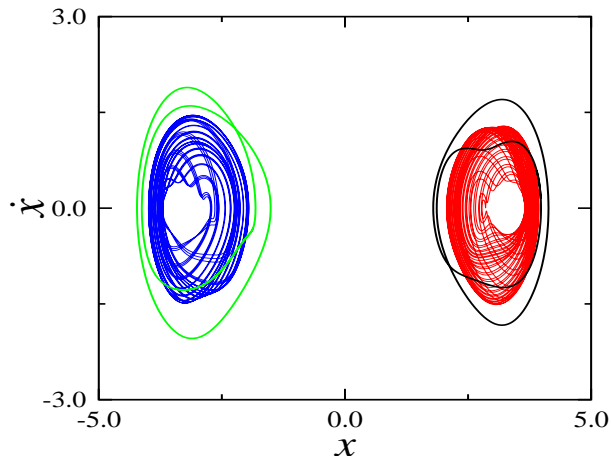

Figure 7: (Color online) Phase portrait of velocity *versus* displacement of four coexisting attractors for the parameters $\alpha = 3.25$ and $\varepsilon = 0.13$. Two periodic attractors plotted in green and black, two quasi-periodic in blue and red.

5. Conclusions

We characterized the non-ideal Duffing oscillator in bi-parameter space, considering the mass ratio, ε, (mechanical coupling parameter) and the source of energy, α. When the source of energy was included, we were able to observe parameter regions identified as Arnold tongues corresponding to mode locked and periodic motion with a common frequency. The mode locked occurs when the combined motion presented in the mass-spring-pendulum driven by a DC motor becomes periodic. We have verified that locked and unlocked regions were interwoven in parameter space. For organization of Arnold tongues, we evaluated the period of the attractors identifying a period-adding cascades and Fibonacci-like sequences. In addition, we identified shrimp-shaped structures immersed in regions of parameter space with chaotic regimes. Exploring an interesting property for this kind of structure, we evaluated the periodicity of the shrimps verifying the important signature of period-3x windows. In other words, the period of the secondary shrimps is three times of the main shrimp.

Furthermore, we have observed, for regions compouding the peripheral part of the tongues (histerese area), coexistence of multiple attractors with intertwined basins of attraction. These basins possess a peculiar structure in which regions composed of complex shape with boundaries convoluted and apparently fractal present subregions inside where the boundary is smooth.

In the end, it is important to emphasize that the characterization of the attractors in parameter space of applied systems is useful to choose robust periodic orbits and also to evaluate the attractor changes in case of controlling chaotic oscillations.
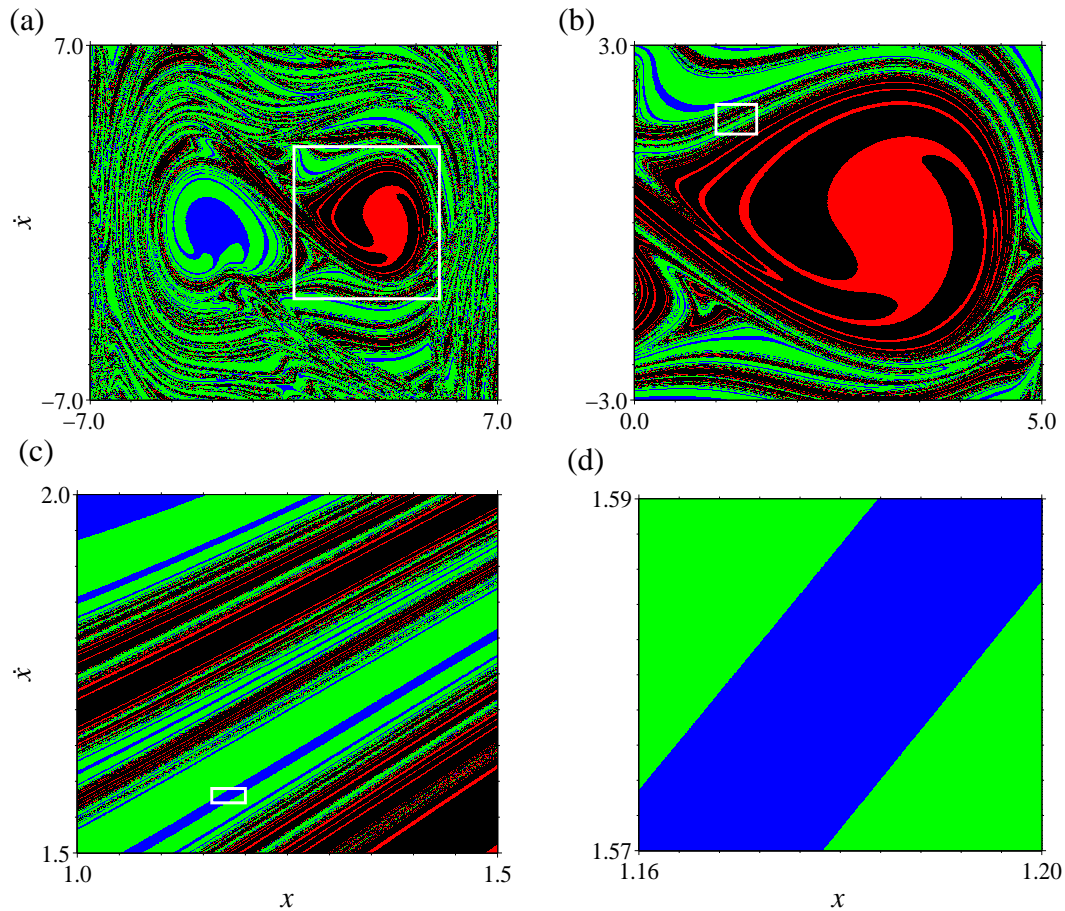
Figure 8: (Color online) Basins of attraction for the attractors shown in Fig. 7 and successive magnifications of boxes in white for the parameters $\alpha = 3.25$ and $\varepsilon = 0.13$, varying initial conditions $\dot{x}$ and x with $\dot{\varphi} = 0.0$ and $\varphi = 0.0$.

Acknowledgments

References

[1] J.A.C. Gallas, Structure of the parameter space of the Hénon map, Phys. Rev. Lett. 70 (1993) 2714-2717.

[2] J.A.C. Gallas, Dissecting shrimps: results for some one-dimensional physical models, Physica A 202 (1994) 196-223.

[3] R.E. Ecke, J.D. Farmer, D.K. Umberger, Scaling of Arnold Tongues, Nonlinearity 2 (1989) 175-196.

[4] H. Jan, K.-T. Tsai, L.-W. Kuo, Phase locking route behind complex periodic windows in a forced oscillator, Chaos 23 (2013) 033126.

[5] F.A.C. Pereira, M.S. Baptista, J.C. Sartorelli, Sound synchronisation of bubble trains in a viscous fluid: Experiment and modelling, Phys. Rev. E 90 (2014) 041902.

[6] S.L.T. de Souza, A.A. Lima, I.L. Caldas, R.O. Medrano-T., Z.O. Guimares-Filho, Self-similarities of periodic structures for a discrete model of a two-gene system, Phys. Lett. A 376 (2012) 1290-1294.

[7] S.L.T. de Souza, I.L. Caldas, R.L. Viana, Multistability and self-similarity in the parameter-space of a vibro-impact system, Math. Probl. Eng. 2009 (2009) 290356.

[8] E.S. Medeiros, S.L.T. de Souza, R.O. Medrano-T., I.L. Caldas, Periodic window arising in the parameter space of an impact oscillator, Phys. Lett. A 374 (2010) 2628-2635.

[9] M. Hansen, D.R. da Costa, D.F.M. Oliveira, E.D. Leonel, Statistical properties for a dissipative model of relativistic particles in a wave packet: A parameter space investigation, Appl. Math. Comput. 238 (2014) 387-392.

[10] C. Stegemann, P.C. Rech, Organization of the dynamics in a parameter plane of a tumor growth mathematical model, Int. J. Bifurcat. Chaos 24 (2014) 1450023.

[11] M.S. Baptista, T.P. Silva, J.C. Sartorelli, I.L. Caldas, Phase synchronization in the perturbed Chua circuit, Phys. Rev. E 67 (2003) 056212.

[12] H.A. Albuquerque, R.M. Rubinger, P.C. Rech, Self-similar structures in a 2D parameter-space of an inductorless, Chua's circuit Physics Letters A 372 (2008) 4793-4798.

[13] A. Hoff, D.T. da Silva, C. Manchein, H.A. Albuquerque, Bifurcation structures and transient chaos in a four-dimensional Chua model, Phys. Lett. A 378 (2014) 171-177.

[14] C. Rosa, M.J. Correia, P.C. Rech, Arnold tongues and quasiperiodicity in a preypredator model, Chaos Soliton. Frac. 40 (2009) 2041-2046.

[15] J. Slipantschuk, E. Ullner, M.S. Baptista, M. Zeineddine, M. Thiel, Abundance of stable periodic behavior in a Red Grouse population model with delay: A consequence of homoclinicity, Chaos 20 (2010) 045117.

[16] I. Iliuk, R.M.L.R.F. Brasil, J.M. Balthazar, A.M. Tusset, V. Piccirillo, J.R.C. Piqueira, Potential application in energy harvesting of intermodal energy exchange in a frame: FEM analysis, Int. J. Struct. Stab. Dy. 14 (2014) 1440027.

[17] S. Lenci, G. Rega, Experimental versus theoretical robustness of rotating solutions in a parametrically excited pendulum: A dynamical integrity perspective, Physica D 204 (2011) 814-824.

[18] J.P. Chávez, M. Wiercigroch, Bifurcation analysis of periodic orbits of a non-smooth Jeffcott rotor model, Commun. Nonlinear Sci. Numer. Simul. 18 (2013) 2571-2580.

[19] Yang Liu, E. Pavlovskaia, D. Hendry, M. Wiercigroch, Vibro-impact responses of capsule system with various friction models, Int. J. Mech. Sci. 72 (2013) 39-54.

[20] L.C. Silva, M.A. Savi, A. Paiva, Nonlinear dynamics of a rotordynamic nonsmooth shape memory alloy system, J. Sound Vibration 332 (2013) 608-621.

[21] H. Sheheitli, R.H. Rand, Dynamics of three coupled limit cycle oscillators with vastly different frequencies, Nonlinear Dynam. 64 (2011) 131-145.

[22] B. Banerjee, A.K. Bajaj, P. Davies, Resonant dynamics of an autoparametric system: a study using higher-order averaging, Int. J. Non Linear Mech. 31 (1996) 21-39.

[23] R. Svoboda, A. Tondl, F. Verhulst, Autoparametric resonance by coupling of linear and non-linear systems, Int. J. Non Linear Mech. 29 (1994) 225-232.

[24] J. Warminski, K. Kecik, Autoparametric vibrations of a nonlinear system with pendulum, Math. Probl. Eng. 2006 (2006) 80705.

[25] R. Almong, S. Zaitsev, O. Shtempluck, E. Buks, Signal amplification in a nanomechanical Duffing resonator via stochastic resonance, Appl. Phys. Lett. 90 (2007) 013508.

[26] J. Suhardjo, B.F. Spencer Jr., M.K. Sain, Nonlinear optimal control of a Duffing system, Int. J. Non Linear Mech. 27 (1992) 157-172.

[27] J.M. Balthazar, D.T. Mook, H.I. Weber, R.M.L.R.F. Brasil, A. Fenili, D. Belato, J.L.P. Felix, An Overview on Non-Ideal Vibrations, Meccanica 38 (2003) 613-621.

[28] P.J.P. Gonçalves, M. Silveira, B.R. Pontes Junior, J.M. Balthazar, The dynamic behavior of a cantilever beam coupled to a non-ideal unbalanced motor through numerical and experimental analysis, J. Sound Vibration 333 (2014) 5115-5129.

[29] S.L.T. de Souza, I.L. Caldas, R.L. Viana, J.M. Balthazar, R.M.L.R.F. Brasil, Dynamics of vibrating systems with tuned liquid column dampers and limited power supply, J. Sound Vibration 289 (2006) 987-998.

[30] S.L.T. de Souza, I.L. Caldas, R.L. Viana, J.M. Balthazar, R.M.L.R.F. Brasil, A simple feedback control for a chaotic oscillator with limited power supply, J. Sound Vibration 299 (2007) 664-671.

[31] S.L.T. de Souza, I.L. Caldas, R.L. Viana, J.M. Balthazar, Control and chaos for vibro-impact and non-ideal oscillator, J. Theor. Appl. Mech. 46 (2008) 641-664.

[32] A.M. Tusset, J.M. Balthazar, On the chaotic suppression of both ideal an non-ideal Duffing based vibrating systems, using a magnetorheological damper, Differential Equations Dynam. Systems 21 (2013) 105-121.

[33] U. Feudel, L. Poon, C. Grebogi, J.A. Yorke, Dynamical properties of a simple mechanical system with a large number of coexisting periodic attractors, Chaos Soliton. Frac. 9 (1998) 171-180.

[34] A.S. Paula, M.A. Savi, F.H.I. Pereira-Pinto, Chaos and transient chaos in an experimental nonlinear pendulum, J. Sound Vibration 294 (2006) 585-595.

[35] E.G. Gwinn, R.M. Westervelt, Fractal basin boundaries and intermittency in the driven damped pendulum, Phys. Rev. A 33 (1986) 4143-4155.

[36] A. Alasty, R. Shabani, Chaotic motions and fractal basin boundaries in spring-pendulum system, Nonlinear Anal. Real World Appl. 7 (2006) 81-95.

[37] S.L.T. de Souza, I.L. Caldas, R.L. Viana, A.M. Batista, T. Kapitaniak, Noise-induced basin hopping in a gearbox model, Chaos Soliton. Fract. 26 (2005) 1523-1531.

[38] S.L.T. de Souza, A.M. Batista, I.L. Caldas, R.L. Viana, T. Kapitaniak, Noise-induced basin hopping in a vibro-impact system, Chaos Soliton. Fract. 32 (2007) 758-767.

[39] A. Wolf, J.B. Swift, H.L. Swinney, J.A. Vastado, Determining Lyapunov exponents from a time series, Physica D 16 (1985) 285-317.

[40] J. Aguirre, R.L. Viana, M.A.F. Sanjun, Fractal structures in nonlinear dynamics, Rev. Mod. Phys. 81 (2009), 333-386.

[41] C. Gebogi, E. Kostelich, E. Ott, J.A. Yorke, Multi-dimensioned intertwined basin boundaries: basin structure of the kicked double rotor, Physica D 25 (1987) 347-360.

[42] X. Xu, M. Wiercigroch, M.P. Cartmell, Rotating orbits of a parametrically-excited pendulum, Chaos Soliton. Fract. 23 (200) 1537-1548.